The Wigner-Boltzmann Monte Carlo Method Applied to Electron Transport in the Presence of a Single Dopant

J.M. Sellier*[a], I. Dimov[a]

[a] *IICT, Bulgarian Academy of Sciences, Acad. G. Bonchev str. 25A, 1113 Sofia, Bulgaria*
* *jeanmichel.sellier@parallel.bas.bg, jeanmichel.sellier@gmail.com*

Abstract

The Wigner-Boltzmann model is a partial integro-differential equation which describes the time dependent dynamics of quantum mechanical phenomena including the effects of lattice vibration as a second-order approximation. Recently a Monte Carlo technique exploiting the concept of signed particles has been developed for its ballistic counterpart, in one and two-dimensional space. In this work, we introduce an extension to the Wigner-Boltzmann model in three-dimensional geometries adapted for the treatment of the scattering term. As an application, we study the dynamics of an electron wave packet in proximity of a Coulombic potential in the presence of absorbing boundary conditions. This mimics the presence of a dopant atom burried in a semiconductor substrate. By using this method, one can observe how the lattice temperature eventually affects the dynamics of the wave packet.

Keywords: Wigner-Boltzmann equation, Monte Carlo methods, Full Quantum Transport, Electron Dynamics, Single Dopant Devices

1. Introduction

The continuous miniaturization of semiconductor devices has reached the point where active lengths are of the order of only several tens of nanometers. At that scale, quantum effects are dominant and classically designed transistors do not operate reliably any longer. The post-CMOS (complementary metal-oxide-semiconductor) era is now a reality. While this represents the end of a very successful period for the semiconductor industry, it is also an opportunity for the development of drastically different device architectures [1], [2], [3]. A shift of design paradigm is now necessary where devices have not to work *despite* the presence of quantum effects, but *because* of them. Recently, a new class of silicon based devices exploiting single burried phosphorus atoms (single dopants) have been presented [4], [5]. While the experiments are advancing quickly [6], [7], [8], going from one single dopant to several dopants placed with atomistic precision [9], the theoretical comprehension of the electron dynamics in such devices is still

in its infancy. Indeed the new paradigm comes with incredible challenges. For meaningful simulations of post-CMOS devices, a model is expected to be time-dependent, fully quantum, capable of including the lattice vibration and, finally, able to deal with open leads. From this perspective, the Wigner-Boltzmann equation represents a promising mathematical tool. It is based on the Wigner equation [10] augmented by the Boltzmann scattering term [11], a second-order approximation model for phonon scattering based on the Fermi golden rule. In this formalism, the evolution of the system is described by an intuitive quasi-distribution function defined on the phase-space, $f_W = f_W(\mathbf{x}, \mathbf{k}, t)$. The price to pay for such model is the appearance of negative values in f_W, a clear signature of quantum mechanical effects. Furthermore, the resolution of the Wigner-Boltzmann equation constitutes an incredible numerical challenge [12].

Despite these difficulties, there has been a very early initial interest in using this formalism for self-consistent calculations based on finite difference techniques [13] which introduce serious problems in the treatment of the diffusion term $\frac{\hbar \mathbf{k}}{m^*} \cdot \nabla_{\mathbf{x}} f_W$. Indeed, the Wigner quasi-distribution function oscillates rapidly in the phase-space causing severe problems in the calculation of the derivatives [14]. A further severe obstacle has been represented by the implementation of injecting boundary conditions (BCs) [15], necessary for self-consistent calculations, a difficult problem not yet solved as recently pointed out [16]. While one can avoid the use of injecting BCs, when self-consistency is not required, the treatment of the diffusion term still remains a problem. Recently, several new approaches, based on Monte Carlo (MC) techniques, have been developed which totally avoid the problem of evaluating the diffusion term. The first attempts [17], [18], [19], [12] are ensemble MC techniques based on the concept of particle affinity. Despite the initial success, it has become rapidly clear that this approach can hardly be applied to multi-dimensional simulations due to the demand of significant computational resources. In fact, the number of particle states in the ensemble inevitably increases during the simulation [12]. Then, a second method, based on the concept of signed particles (appearing for the first time in the context of stationary calculations relying on the ergodicity of the problem determined by the BCs [20]) has been introduced [21], [22]. This method is based on the Iterative MC method for solving linear and non-linear equations (both integral and algebraic) [23], [24] applied to the Wigner equation. It is a time-dependent approach which can take into account general initial conditions along with general BCs. This relatively new technique allows time dependent, full quantum and multi-dimensional simulations for acceptable computational time and resources.

In this work we generalize the signed particles Wigner MC method to the Wigner-Boltzmann equation in order to take into account the Boltzmann collision term modelling the scattering with phonons. As a practical example, we perform three-dimensional (3D) simulations of a wave packet moving in a semiconductor substrate in the presence of a Coulombic potential. We utilize only reflective and absorbing BCs (which are time-irreversible and in agreement with [15]) since no self-consistency is required in this particular numerical experiment. This shows how different lattice temperatures affect the evolution of the

system. This paves the way towards time dependent, multi-dimensional, full quantum TCAD (Technology Computer Aided Design) tools, able to include (yet to some extent) the effects of lattice vibration, for the next generation of electronic post-CMOS devices.

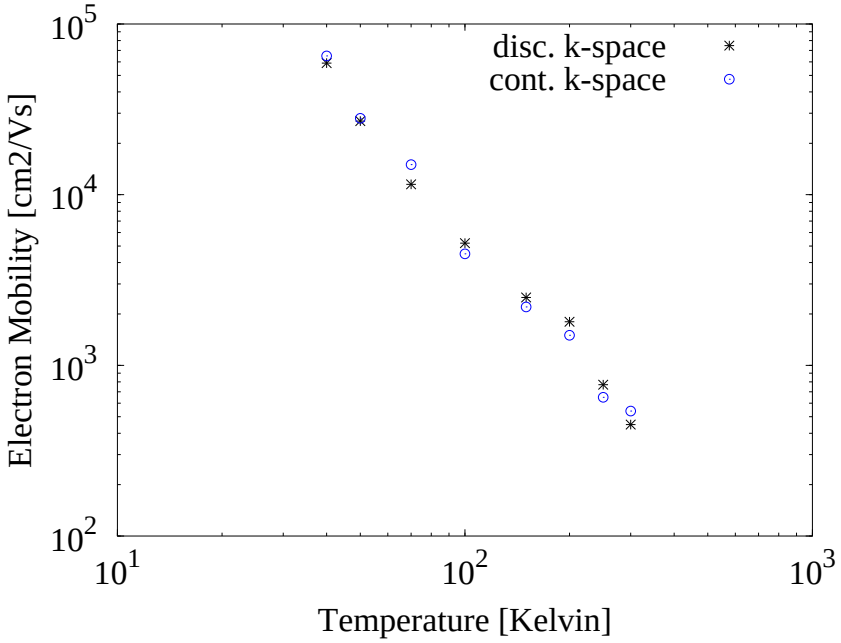

Figure 1: Low-field electron mobility calculated for bulk silicon at temperatures ranging from 40 K to 300 K. The $*$ symbols show the mobility calculated using a discretized wave-space, while the o symbols show the mobility calculated by means of a continuous wave-space. The impurity scattering is not taken into account.

2. The Wigner-Boltzmann Monte Carlo method

In a continuous phase-space and in the Bloch formalism, the Wigner-Boltzmann equation reads

$$\frac{\partial f_W}{\partial t} + \frac{\hbar \mathbf{k}}{m^*} \cdot \nabla_{\mathbf{x}} f_W = Q_W\left[f_W\right] + C_B\left[f_W\right], \tag{1}$$

where $f_W = f_W(\mathbf{x}, \mathbf{k}, t)$ is the unknown pseudo-distribution function defined over the 7-dimensional phase-space $(\mathbf{x}, \mathbf{k}, t) = (x, y, z, k_x, k_y, k_z, t)$, m^* is the effective mass, Q_W is a functional defined as

$$Q_W\left[f_W\right](\mathbf{x}, \mathbf{k}, t) = \int d\mathbf{k}' V_W(\mathbf{x}, \mathbf{k} - \mathbf{k}', t) f_W(\mathbf{x}, \mathbf{k}, t),$$

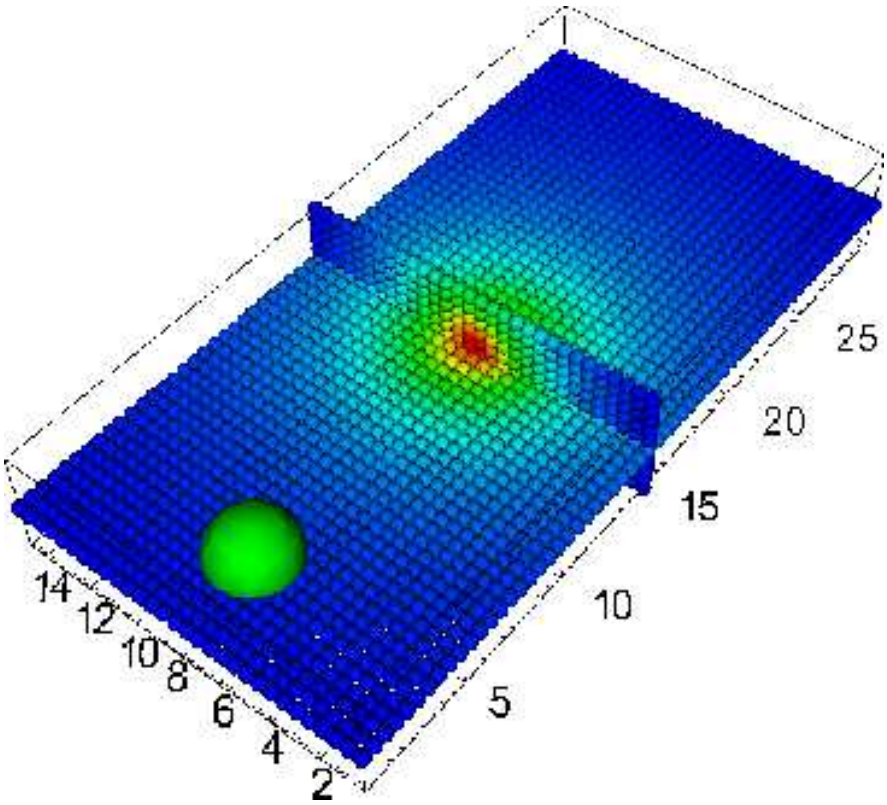

Figure 2: Initial Gaussian wave packet: isosurface corresponding to 50% of finding an electron (calculated from the normalized Wigner distribution function). The unit for coordinates is nanometer.

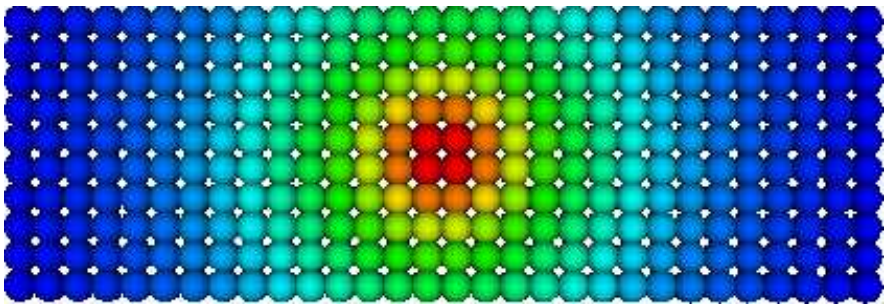

Figure 3: Transversal cut of the Coulombic electrostatic potential due to a phosphorus dopant (the spheres represent magnified centers of the grid cells).

the Wigner potential is defined as

$$V_W(\mathbf{x},\mathbf{k},t) = \frac{1}{i\hbar 8\pi^3}\int d\mathbf{x}' e^{-i\mathbf{k}\cdot\mathbf{x}'}\left[V(\mathbf{x}+\frac{\mathbf{x}'}{2},t) - V(\mathbf{x}-\frac{\mathbf{x}'}{2},t)\right], \qquad (2)$$

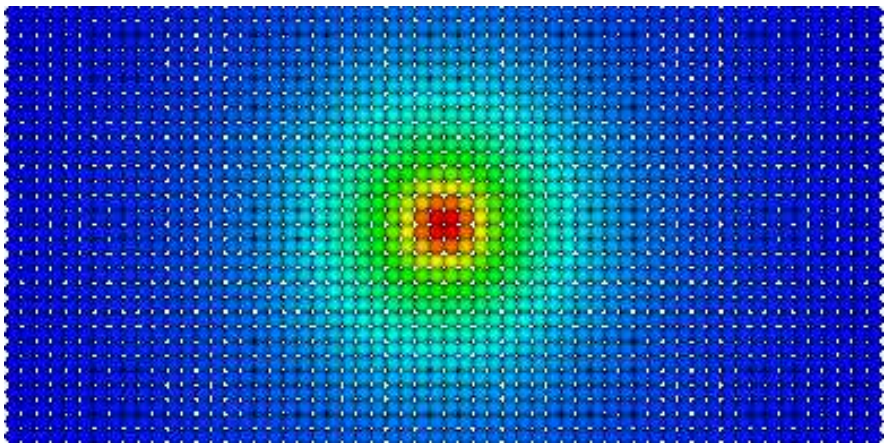

Figure 4: Longitudinal cut of the Coulombic electrostatic potential due to a phosphorus dopant (the spheres represent magnified centers of the grid cells).

and the Boltzmann collision term is defined as [11]

$$C_B\left[f_W\right](\mathbf{x},\mathbf{k},t) = \sum_i \int_{-\infty}^{+\infty} d\mathbf{k}' \left[S_i(\mathbf{k}',\mathbf{k}) f_W(\mathbf{x},\mathbf{k}',t) - S_i(\mathbf{k},\mathbf{k}') f_W(\mathbf{x},\mathbf{k},t)\right],$$

where the kernel $S_i = S_i(\mathbf{k},\mathbf{k}')$ takes into account the $i-th$ scattering process between electrons and phonons (e.g. optical , acoustic, etc). In particular, the kernel $S_i(\mathbf{k},\mathbf{k}')$ is calculated from the Fermi golden rule [11] and it can be shown that the Wigner-Boltzmann equation (1) makes perfectly physical sense under conditions which are not too restrictive [12]. Finally, one should note that scattering terms beyond the Boltzmann formalism nowadays exist [25], but in this work, for the sake of simplicity, we use the Boltzmann term limiting ourselves to a semi-classical treatment of phonon scattering events.

By following the method depicted in [22], the Wigner-Boltzmann model is rewritten exploiting the semi-discrete nature of the phase-space. Indeed, on one side, physical considerations show that the simulation domain for the quantum structure is bounded by an upper limit $\mathbf{L}_C = (L_C^x, L_C^y, L_C^z)$ known as the coherence length. On the other side, particle energy comes in quanta. From these considerations, one can express the k-space in terms of multiples of a finite quantity $\Delta\mathbf{k} = \frac{\pi}{\mathbf{L}_C}$. In other words, a discretization of the k-space is introduced. Thus, in the rest of the paper, we express the wave vector of a particle as a set of 3 integers and denote it as $\mathbf{M} = (M_x, M_y, M_z)$. This corresponds to a wave vector $\mathbf{k} = \mathbf{M}\Delta\mathbf{k} = (M_x \times \Delta k_x, M_y \times \Delta k_y, M_z \times \Delta k_z)$. The Wigner-Boltzmann equation, in a semi-discrete phase-space, reads

$$\frac{\partial f_W}{\partial t}(\mathbf{x},\mathbf{M}) \quad + \quad \frac{\hbar}{m^*}\mathbf{M}\Delta\mathbf{k}\cdot\nabla_{\mathbf{x}} f_W(\mathbf{x},\mathbf{M})$$

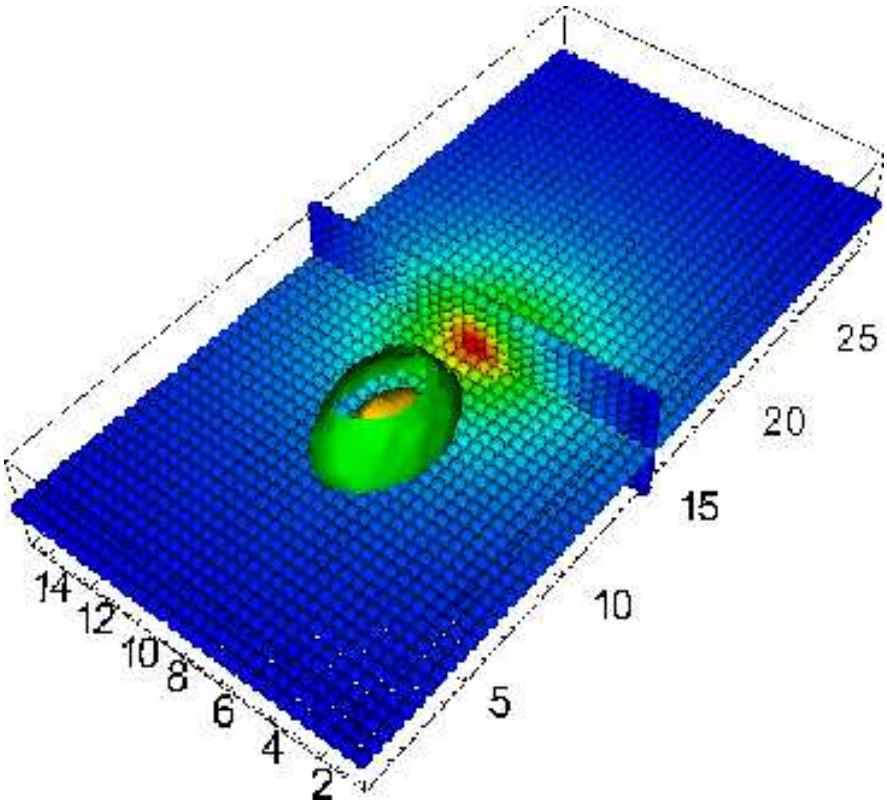

Figure 5: Evolution of a wave packet at time 10 fs with initial energy equal to 0.42 eV and lattice temperature 20 mK. Two isosurfaces are shown corresponding to 50% (external green surface) and 80% (internal yellow surface).

$$= \sum_{\mathbf{N}=-\infty}^{+\infty} V_W\left(\mathbf{x}, (\mathbf{M}-\mathbf{N})\right) f_W(\mathbf{x},\mathbf{N}) + C_B\left[f_W(\mathbf{x},\mathbf{M})\right] \quad (3)$$

and the Wigner potential and the Boltzmann scattering terms are reformulated accordingly

$$V_W(\mathbf{x},\mathbf{M},t) = \frac{1}{i\hbar\mathbf{L}_C}\int_{-\mathbf{L}_C/2}^{+\mathbf{L}_C/2} d\mathbf{x}' e^{-i2\mathbf{M}\Delta\mathbf{k}}\left(V(\mathbf{x}+\mathbf{x}',t) - V(\mathbf{x}-\mathbf{x}',t)\right),$$

$$C_B\left[f_W\right](\mathbf{x},\mathbf{M},t) = \sum_i \sum_{N=-\infty}^{+\infty}\left[S_i(\mathbf{N},\mathbf{M}) f_W(\mathbf{x},\mathbf{N},t) - S_i(\mathbf{M},\mathbf{N}) f_W(\mathbf{x},\mathbf{M},t)\right].$$

A time dependent MC method to solve the ballistic part of the semi-discrete Wigner-Boltzmann equation (3) has been recently presented in [21] and [22] based on the Iterative MC method presented in [23], [24] All technical details are reported in the above references and we hereby sketch them only briefly.

A quantity $\gamma = \gamma(\mathbf{x})$, obtained from the Wigner potential, is defined [22] and a particle generation process is introduced [23], [24]. During its free flight, an initial signed particle creates a pair of new particles, one positive and the other negative. If, initially, the parent particle has a sign s, a position $\mathbf{x}$ and a wave-vector $\mathbf{M}$, it generates, with a given rate depending on the Wigner potential, a pair of new particles with signs s, $-s$, position $\mathbf{x}$ (both are in the same position of the parent particle) and momenta $\mathbf{M}' = \mathbf{M} + \mathbf{N}$, $\mathbf{M}' = \mathbf{M} - \mathbf{N}$ respectively. After the creation event, the parent particle continues its free flight evolution until a given time T and the new pair of particles is evolved in the same way. One should note that the signed particles evolve over field-less Newtonian trajectories and contribute to the values of the physical averages only by their sign. In other words, the action of the Wigner potential on a signed particle happens only by generation of particles following certain rules. Thus, the time-dependent evolution of the Wigner quasi-distribution happens only by creation and annihilation of particles which replace the acceleration due to Newtonian forces [21], [22]. Finally, we stress on the fact that these Newtonian particles are only a constructive mathematical tool (sometimes called *virtual* particles in the Monte Carlo theory) and, as such, they allow us to apply general boundary conditions in a natural way. This method has been validated with success against one-dimensional, two-dimensional benchmark tests and technologically relevant situations [21], [22], [26], [27].

Now, in order to include the Boltzmann collision term in a full quantum simulation, one starts from the fact that particles constituting the Wigner MC method are Newtonian objects. By supposing that the total simulation time T has been divided in intervals equal to ΔT, our problem consists of including the phonon scattering events during these intervals. To achieve such goal, we follow a technique similar to the one implemented in the Boltzmann MC method [11] but adapted to the *discreteness* of the wave-space and evolving particles on free-flight trajectories as *signed* quantum particles. It is well-known that, in the semiclassical approach, the system is represented by an ensemble of pseudo-particles (essentially weighted particles which mimic physical electrons). The dynamics of such pseudo-particles happens in two phases, i.e. a drift or free-flight evolution and a scattering event, which are repeated until time ΔT is reached. Now, in order to include the quantum nature of the problem, the system is described in terms of signed particles which free-flight evolution strictly follows the dynamics depicted in the Wigner MC algorithm [22]. In other words, during every free-flight interval, the particle is evolved as a signed particle, i.e. it creates new pairs of signed particles and moves in its field-less Newtonian trajectory. When the parent particle reaches the end of the free flight interval, its discrete momentum $\mathbf{M}$ is updated. Furthermore, being the wave-space now discrete, the probability $P[\mathbf{M}(t)]$ utilized to compute the free-flight duration is accordingly modified and reads

$$P[\mathbf{M}] = \sum_i \sum_{\mathbf{N}=-\infty}^{+\infty} S_i(\mathbf{M}, \mathbf{N}). \tag{4}$$

Finally, the newly created pairs are evolved in the same fashion, i.e. signed particles, and the process goes ahead until all particles are evolved. An algorithm is reported below for the sake of clarity.

```
for particle i
   . given the interval DT
   . compute the free flight interval dt
   for free flight dt
      . evolve particle i as a signed particle,
      . generate signed particles, etc.
      . add the new particles to the existing ensemble of particles
   end
   . update the momentum of particle i
end
```

We now proceed with a benchmark test and applications of the Wigner-Boltzmann MC method to practical situations.

3. Electron mobility in bulk silicon

In order to assess the reliability of the proposed Wigner-Boltzmann MC method, we numerically investigate the use of the probability (4) for the inclusion of the phonon scattering events in a discretized wave-space. Indeed, it is important to show that the discretization does not introduce any spurious numerical effect such as, for example, artificial heating. To this goal, we perform a benchmark test consisting of calculating the electron mobility in bulk silicon in the presence of non-polar optical and acoustic phonons by means of a single-particle MC method [11] which, essentially, involves the evolution of a particle in the wave-space only. In this test, the ionized impurity scattering event is neglected in order to focus on the effect of the lattice temperature.

The continuous probabilities utilized in our calculations are defined in the parabolic band approximation. The non-polar optical term reads

$$P_{opt}(k) = \frac{\pi D_i^2 Z_i}{\rho \omega_i} \left[n_i + \frac{1}{2} \mp \frac{1}{2} \right] N(\frac{\hbar^2 k^2}{2m^*} \pm \hbar\omega_i), \tag{5}$$

where $i = 1, \ldots, 6$, $m^* = 0.32 m_0$, m_0 the electron mass, D_i is the optical deformation potential, Z_i is the number of final valleys available for scattering, $\hbar\omega_i$ is the energy of the optical phonon, ρ is the crystal density, N is the density of states and n_i is the occupation number. The acoustic term reads

$$P_{ac}(k) = \frac{\Xi_d^2 k_B T_L}{\hbar c_L} \frac{m^* k}{\pi \hbar^2}, \tag{6}$$

where Ξ_d is the acoustic deformation potential, k_B is the Boltzmann constant and c_L is the longitudinal sound velocity. The values for the parameters in (5) and (6) are taken from [28].

The calculation of the electron mobility is first carried out utilizing the *continuous* probability of the semiclassical Boltzmann MC method (5), (6) and, then, by means of the *discretized* probability (4) introduced in the Wigner MC method. In both calculations, a single particle is evolved in the k-space until 5 ps and the mobility is calculated utilizing the mean carrier velocity. The temperatures involved are in the range $[40; 300]$ K and, in the Wigner MC case, the wave-space corresponds to an energy range $[0; 0.5]$ eV discretized over 200 cells.

The comparison between the continuous and discretized wave-space is shown in Fig. 1 (o continuous and $*$ discrete cases respectively) where a good agreement is obtained. One should note that this agreement is, of course, achievable only if a refined enough wave mesh is selected. Indeed, if the wave-space discretization is too coarse then the energy difference between two adjacent wave-vectors quickly becomes too big and phonon scattering is either underestimated or overestimated. We can now proceed to apply the Wigner-Boltzmann MC method to a practical situation.

4. Simulation of single-dopant systems

In this section, we perform two 3D numerical experiments involving the evolution of an electron wave packet in proximity of a positive Coulombic potential. This mimics the presence of a phosphorus atom embedded in silicon substrate. We include scattering events with non-polar optical phonons and acoustic phonons [11] and analyse how the probability of finding an electron is affected by the lattice temperature at 20 mK (ballistic regime, i.e. scattering events switched off) and 300 K (room temperature, i.e. scattering events switched on). In order to simplify the problem, the electron is supposed to enter from one lead (left-hand side) with a longitudinal component only. If the particle is absorbed by the second lead (right-hand side) then a peak in the current profile appears. Our aim is to demonstrate that, utilizing the Wigner-Boltzmann MC method, the development of practical TCAD tools to understand and design electronic devices exploiting quantum effects is a feasible task.

4.1. Description

The initial conditions for these experiments consist of a Gaussian wave packet with minimal uncertainty (see Fig.2). The corresponding initial conditions in the Wigner formalism read:

$$f_W^0(\mathbf{x}, \mathbf{m}) = A_N e^{-\frac{(\mathbf{x}-\mathbf{x}_0)^2}{\sigma^2}} e^{-(\mathbf{m}\Delta\mathbf{k}-\mathbf{k}_0)^2\sigma^2}, \tag{7}$$

where A_N, $\mathbf{k}_0$, $\mathbf{x}_0$ and σ are, respectively, a constant of normalization, the initial wave vector, the initial position, and the dispersion of the wave packet. The value for σ is 2 nm while the initial position is 3.5 nm. The electron initial wave vector $\mathbf{k}_0$ corresponds to an energy equal to 0.42 eV. Open BCs, which absorb particles, are imposed on the left and right-hand side of the domain. They

are reflective otherwise. The lattice temperature is equal to 20 mK (ballistic regime) in the first experiment and 300 K (room temperature) in the second one. The dimensions of the domain are $30nm \times 15nm \times 5nm$. A positive Coulombic potential is placed at the center which mathematically reads

$$V(\mathbf{x}) = \frac{q}{4\pi\epsilon_0\epsilon_r \left(\mathbf{x}^2 + \frac{1}{2}r_c^2\right)^{\frac{1}{2}}}, \tag{8}$$

where r_c is the Bohr radius in silicon (about 1.93 nm, see Fig.3 and Fig.4) [29]. One expects two kind of processes to happen, i.e. partial reflection and absorption from the Coulombic potential which behaves as a quantum well, and absorption of the packet through the left and right-hand side boundaries.

4.2. Ballistic regime

A high energetic electron (corresponding to about 423 meV) is introduced from the left-hand side of the domain at a temperature equal to 20 mK. The wave packet proceeds towards the center with practically no interaction with the lattice (ballistic regime). The evolution of the simulated system is reported in Fig.5, Fig.6 and Fig.7 for 10 fs, 20 fs and 30 fs respectively. One observes that, in these conditions, the electron is not trapped by the Coulombic potential. Indeed it is too energetic. The electron will, eventually, be absorbed by the right-hand side boundary with a high probability. Indeed, Fig.7 clearly shows that the wave packet is in proximity of the right-hand side lead at 30 fs already. This experiment shows that, in this situation, the wave packet is barely influenced by the presence of the Coulombic potential.

4.3. Room temperature

The aim of this numerical experiment is to show how the lattice temperature greatly affects the dynamics of an electron wave packet even though the involved lenghts and evolution times are very small. We start from the same conditions as the previous experiment where the lattice temperature is now equal to 300 K (corresponding to an energy of about 387 meV). The results of this experiment are shown in Fig.8, Fig.9 and Fig.10 again for times equal to 10 fs, 20 fs and 30 fs respectively. One clearly observes that the wave packet is now feeling the Coulombic potential. In fact, at room temperature, phonon scattering is not a rare event any longer. The electron energy is influenced by the lattice vibration which pushes it to equilibrium. Eventually the electron becomes low energetic and feels the Coulombic potential, indeed the wave packet is now shaped by the presence of the dopant. The electron dynamics is clearly much slower than compared to the previous experiment, as it can be seen by a comparison between Fig.7, where the wave packet is already approaching the right-hand side lead, and Fig.10, where the wave packet still holds in the first half of the device.

5. Computational aspects

The simulator used to obtain the results presented in this paper is a modified version of Archimedes, the GNU package for the simulation of carrier transport in semiconductor devices [30]. This code was first released in 2005, and, since then, users have been able to download the source code under the GNU Public License (GPL). Many features have been introduced in this package. In this particular project, our aim has been to develop a full quantum time-dependent nanodevice simulator including phonon scattering effects. The code is entirely developed in C and optimized to get the best performance from the hardware. It can run on parallel machines using the OpenMP standard library. The results of the present version are posted on the nano-archimedes website, dedicated to the simulation of nanodevices [31].

The results have been obtained using the HPC cluster deployed at the Institute of Information and Communication Technologies of the Bulgarian Academy of Sciences. This cluster consists of two racks which contain HP Cluster Platform Express 7000 enclosures with 36 blades BL 280c with dual Intel Xeon X5560 @ 2.8 Ghz (total 576 cores), 24 GB RAM per blade. There are 8 storage and management controlling nodes 8 HP DL 380 G6 with dual Intel X5560 @ 2.8 Ghz and 32 GB RAM. All these servers are interconnected via non-blocking DDR Infiniband interconnect at 20Gbps line speed. The theoretical peak performance is 3.23 Tflops.

6. Conclusions

In this paper we introduced a Monte Carlo approach for the three-dimensional Wigner-Boltzmann equation based on the concept of signed particles. We applied it to the simulation of a wave packet in proximity of a Coulombic potential. This is similar to a single dopant system consisting of a phosphorus atom buried in a silicon substrate. We have shown how the lattice temperature plays an important role even for very small structures and time scales. We have shown that at room temperature the lattice vibration tends to reduce the electron energy and even relatively high energetic electron wave packets can eventually be shaped by the Coulombic potential. These experiments show that full quantum, time dependent, multi-dimensional TCAD tools for next generation nanoscaled devices exploiting quantum effects are now a reachable task.

Acknowledgements. This work has been supported by the the project EC AComIn (FP7-REGPOT-2012-2013-1).

References

[1] M.V. Fischetti, S.E. Laux, Monte Carlo Simulation of Electron Transport in Si: The First 20 Years, Proceedings of the European Solid State Device Research Conference (ESSDERC 96), (1996) 813-802.

[2] S.M. Reimann, M. Manninen, Electronic Structure of Quantum Dots, Rev. Mod. Phys. 74, (2002) 1283-1342.

[3] K.S. Novoselov, A.K. Geim, S.V. Morozov, D. Jiang, Y. Zhang, S.V. Dubonos, I.V. Grigorieva, A.A. Firsov, Electric Field Effect in Atomically Thin Carbon Films, Science 306, (2004) 666.

[4] B.E. Kane, A Silicon-based Nuclear Spin Quantum Computer, Nature 393 (1998) 133-137.

[5] L.C.L. Hollenberg, A.S. Dzurak, C. Wellard, A.R. Hamilton, D.J. Reilly, G.J. Milburn, R.G. Clark, Charged-based Quantum Computing Using Single Donors in Semiconductors, Phys. Rev. B 69 (2004) 113301.

[6] K. Yokoi, D. Moraru, M. Ligowski, M. Tabe, Single-gated Single-electron Transfer in Nonuniform Arrays of Quantum Dots, Jpn. J. Appl. Phys. 48 (2009) 024503.

[7] E. Hamid, D. Moraru, J.C. Tarido, S. Miki, T. Mizuno, M. Tabe, Single-electron Transfer between Two Donors in Nanoscale Thin Silicon-on-insulator Field-effect Transistors, Apply. Phys. Lett. 97 (2010) 262101.

[8] D. Moraru, A. Udhiarto, M. Anwar, R. Nowak, R. Jablonski, E. Hamid, J.C. Tarido, T. Mizuno, M. Tabe, Atom Devices Based on Single Dopants in Silicon Nanostructures, Nanoscale Research Letters 6 (2011) 479.

[9] M. Simmons, S. Schofield, J. Obrien, N. Curson, L. Oberbeck, T. Hallam, R. Clark, Towards the Atomic-scale Fabrication of a Silicon-based Solid State Quantum Computer, Surface Science (2003) 1209-1218.

[10] E. Wigner, On the Quantum Correction for Thermodynamic Equilibrium, Phys. Rev. 40 (1932) 749.

[11] C. Jacoboni, L. Reggiani, The Monte Carlo Method for the Solution of Charge Transport in Semiconductors with Applications to Covalent Materials, Rev. Mod. Phys 55 (1983) 645.

[12] D. Querlioz, P. Dollfus, The Wigner Monte Carlo Method for Nanoelectronic Devices - A Particle Description of Quantum Transport and Decoherence, ISTE-Wiley, 2010.

[13] U. Ravaioli, M.A. Osman, W. Pötz, N.C. Kluksdahl, D.K. Ferry, Investigation of Ballistic Transport through Resonant Tunneling Quantum Wells Using Wigner Function Approach, Physica B 134 (1985) 36-40.

[14] K.Y. Kim, B. Lee, On the High Order Numerical Calculation Schemes for the Wigner Transport Equation, Solid-State Electr. 43 (1999) 2243-2245.

[15] W.R. Frensley, Boundary conditions for open quantum systems driven far from equilibrium, Rev. Mod.Phys. 62 (1990) 745.

[16] R.Rosati, F. Dolcini, R.C. Iotti, F. Rossi, Wigner-function Formalism Applied to Semiconductor Quantum Devices: Failure of the Conventional Boundary Condition Scheme, Phys. Rev. B 88 (2013) 035401.

[17] L. Shifren, D.K. Ferry, Particle Monte Carlo simulation of Wigner function tunneling, Phys. Lett. A 285 (2001) 217-221.

[18] L. Shifren, D.K. Ferry, A Wigner Function Based Ensemble Monte Carlo Approach for Accurate Incorporation of Quantum Effects in Device Simulation, J. Comp. Electr. 1 (2002) 55-58.

[19] L. Shifren, D.K. Ferry, Wigner Function Quantum Monte Carlo, Physica B 314 (2002) 72-75.

[20] M. Nedjalkov, H. Kosina, S. Selberherr, Ch. Ringhofer, D.K. Ferry, Unified Particle Approach to Wigner-Boltzmann Transport in Small Semiconductor Devices, Phys. Rev. B 70 (2004) 115319.

[21] M. Nedjalkov, P. Schwaha, S. Selberherr, J.M. Sellier, D. Vasileska, Wigner Quasi-Particle Attributes: An Asymptotic Perspective, Appl. Phys. Lett. 102 (2013) 163113.

[22] J.M. Sellier, M. Nedjalkov, I. Dimov, S. Selberherr, A benchmark study of the Wigner Monte-Carlo method, Monte Carlo Methods and Applications, De Gruyter, DOI: 10.1515/mcma-2013-0018, (2014).

[23] I. Dimov, Monte Carlo Algorithms for Linear Problems, Pliska (Studia Mathematica Bulgarica), Vol. 13 (2000), 1997, pp. 57-77.

[24] 18. I. Dimov, T. Gurov, Monte Carlo Algorithm for Solving Integral Equations with Polynomial Non-linearity. Parallel Implementation, Pliska (Studia Mathematica Bulgarica), Vol. 13 (2000), 1997, pp. 117-132.

[25] M. Nedjalkov, D. Vasilevska, D.K. Ferry, C. Jacoboni, C. Ringhofer, I. Dimov, V. Palankovski, Wigner Transport Models of the Electron-phonon Kinetics in Quantum Wires, Phys. Rev. B 74 (2006) 035311.

[26] J.M. Sellier, M. Nedjalkov, I. Dimov, S. Selberherr, The Role of Annihilation in a Wigner Monte Carlo Approach, Proceedings of the International Conference on Large-Scale Scientific Computations (2013) 78.

[27] S. Amoroso, L. Gerrer, A. Asenov, J.M. Sellier, I. Dimov, M. Nedjalkov, S. Selberherr, Quantum Insights in Gate Oxide Charge-Trapping Dynamics in Nanoscale MOSFETs, Proceedings of the 18th International Conference on Simulation of Semiconductor Processes and Devices (2013) 25-28.

[28] K. Tomizawa, Numerical Simulation of Submicron Semiconductor Devices, Artech House, (1993).

[29] R.W. Hockney, J.W. Eastwood, Computer Simulation using particles, A. Hilger, (1988).

[30] J.M. Sellier, GNU Archimedes, accessed 10 Oct. 2013,
URL: www.gnu.org/software/archimedes

[31] J.M. Sellier, nano-archimedes, accessed 10 Oct. 2013,
URL: www.nano-archimedes.com

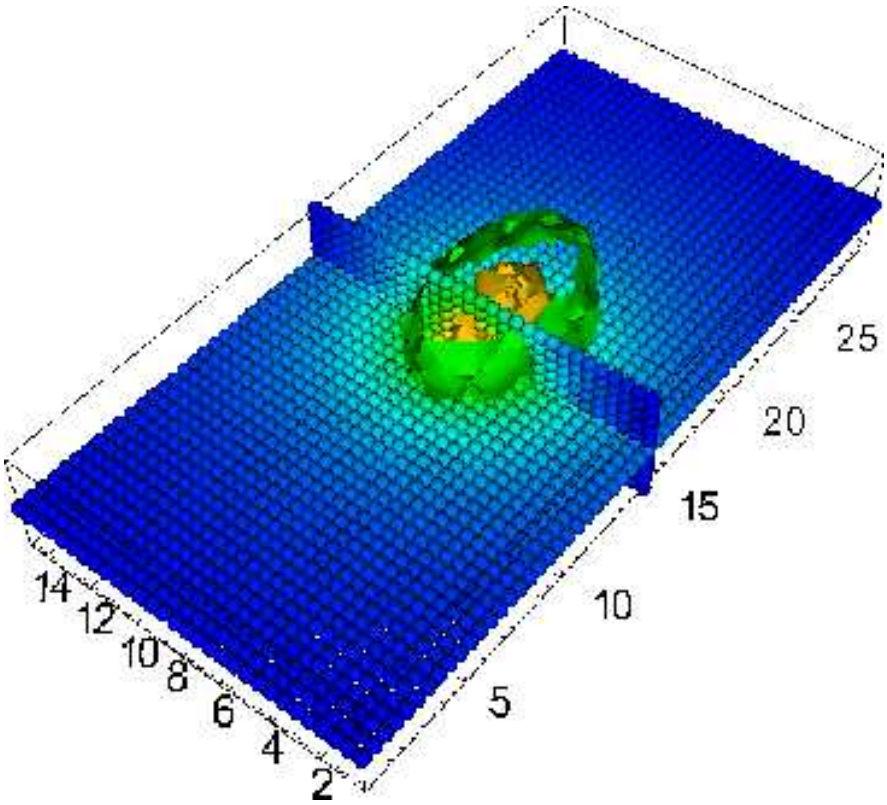

Figure 6: Evolution of a wave packet at time 20 fs with initial energy equal to 0.42 eV and lattice temperature 20 mK. Two isosurfaces are shown corresponding to 50% (external green surface) and 80% (internal yellow surface).

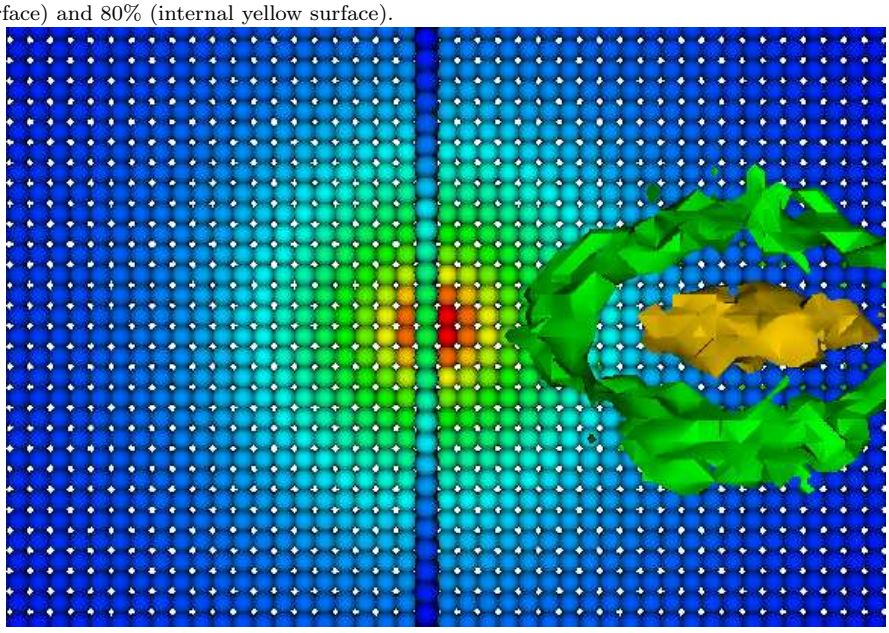

Figure 7: Top view of the evolution of a wave packet at time 30 fs with initial energy equal to 0.42 eV and lattice temperature 20 mK. Two isosurfaces are shown corresponding to 50% (external green surface) and 80% (internal yellow surface). The wave packet is now moving towards the second lead (right-hand side).

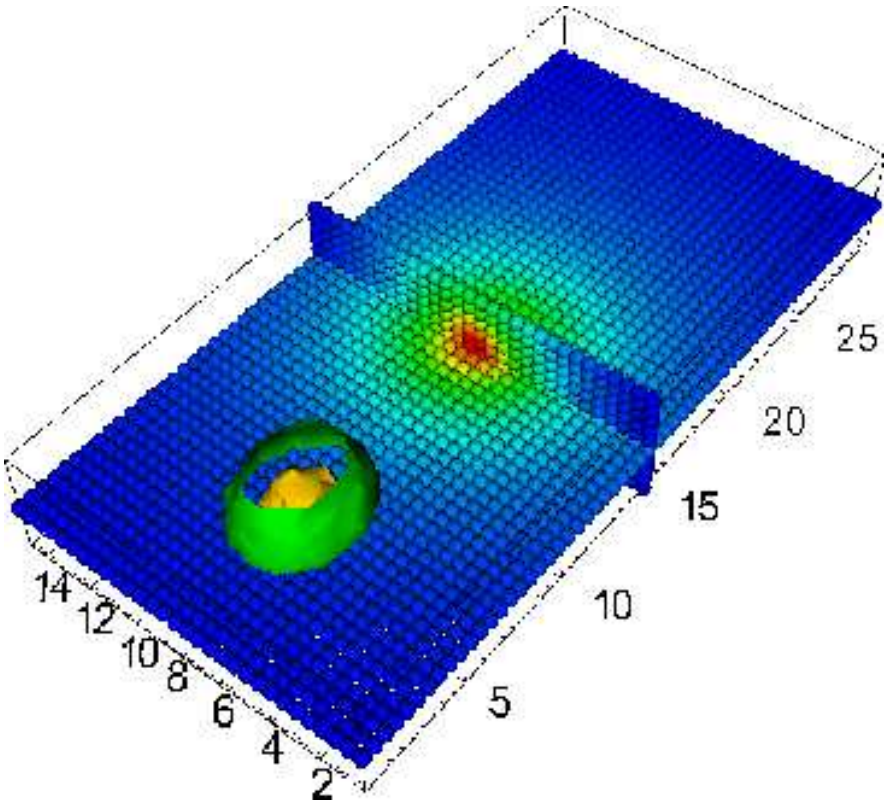

Figure 8: Evolution of a wave packet at time 10 fs with initial energy equal to 0.42 eV and lattice temperature 300 K. Two isosurfaces are shown corresponding to 50% (external green surface) and 80% (internal yellow surface).

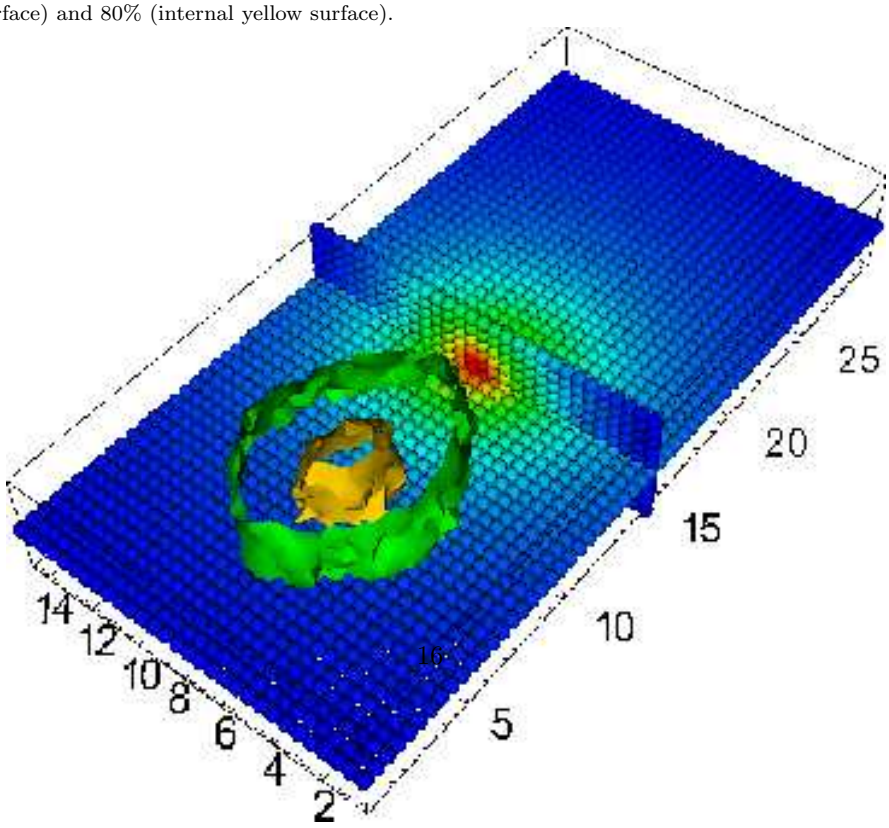

Figure 9: Evolution of a wave packet at time 20 fs with initial energy equal to 0.42 eV and lattice temperature 300 K. Two isosurfaces are shown corresponding to 50% (external green surface) and 80% (internal yellow surface).

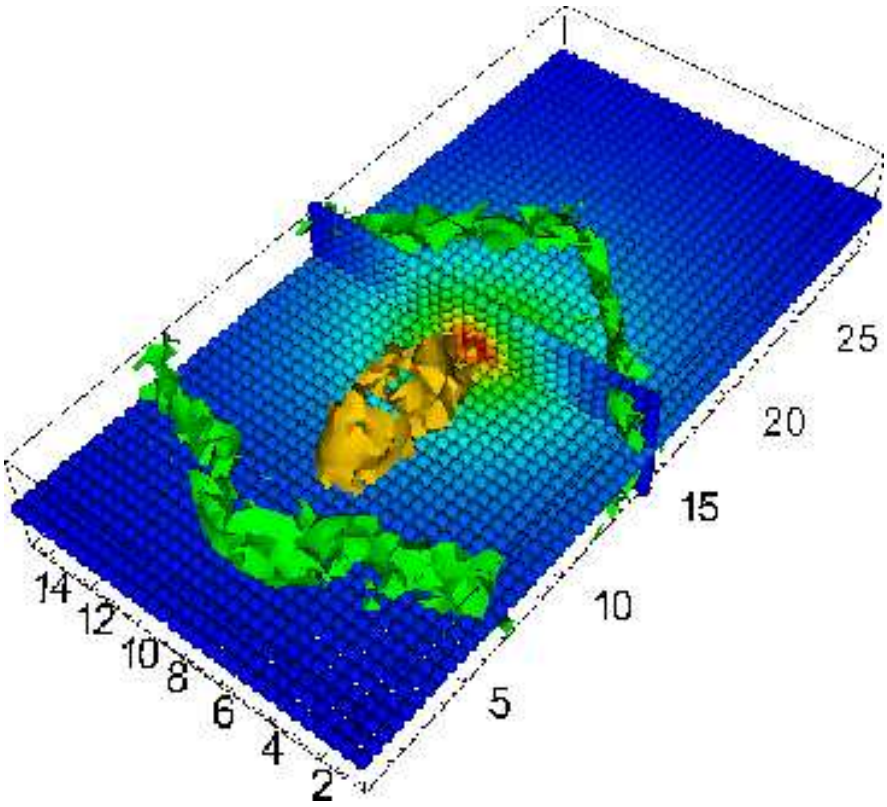

Figure 10: Evolution of a wave packet at time 30 fs with initial energy equal to 0.42 eV and lattice temperature 300 K. Two isosurfaces are shown corresponding to 50% (external green surface) and 80% (internal yellow surface).